

Supporting Information for:

Solvation vs. Surface Charge Transfer: An Interfacial Chemistry Game Drives Cation Motion

Stefany Angarita-Gomez and Perla B. Balbuena*

Department of Chemical Engineering,
Texas A&M University, College Station, TX 77843

*e-mail: balbuena@tamu.edu

Computational methods and system details

Lithium metal slab structure is created using seven layers of lithium metal exposing the lowest surface energy facet (100);¹ the bottom two layers of the slab are fixed to resemble bulk behavior. The total dimensions of the cell including the lithium metal slab are 10.3 Å x 13.8 Å x 33.3 Å. A vacuum layer of ~23 Å added above the Li metal surface in the Z direction, provides the space where the electrolyte is located. A fixed helium layer is added at 3 Å from the top of the cell, to prevent the interaction of the electrolyte with the bottom layers of lithium metal due to the periodic boundary conditions. The initial construction of the cell after the placement of the Li⁺ and PF₆⁻ anion begins with packing

of the appropriate density of the solution (e.g. DME $\rho = 0.87 \frac{g}{cm^3}$, DOL $\rho = 1.06 \frac{g}{cm^3}$ and

EC $= 1.32 \frac{g}{cm^3}$). Relaxation of solvent molecules after the packing is achieved by minimization done via classical molecular mechanics. The minimization with classical mechanics is done using a consistent valence force field (CVFF)² as implemented in the Materials Studio software.

The cells were optimized using the Vienna ab Initio Simulation Package (VASP).³⁻⁵ Electron-ion interactions were described by the projector augmented wave (PAW) pseudopotentials^{6,7} provided in VASP database. The Perdew-Burke-Ernzerhof generalized gradient approximation (GGA-PBE)⁸ was used as exchange-correlation functional. The energy cut-off for the plane-wave basis expansion was chosen to be 400 eV. A conjugate-gradient algorithm was employed to relax the ions into their instantaneous ground state. Gaussian smearing with a width of 0.05 eV was also utilized. For the surface Brillouin zone integration, a 2×2×1 Monkhorst-Pack⁹ k-point mesh was used. The convergence criteria for electronic self-consistent iteration and ionic relaxation were set to 10^{-4} and 10^{-3} eV, respectively.

After the optimization of the cell, thermodynamic integration simulations were carried out using the Blue Moon ensemble method as implemented in VASP. This technique allows us to study the energy barriers involved in the cation diffusion, desolvation and deposition, therefore identify relevant steps during the trajectory. The collective variable (ξ) is defined as the reaction coordinate that defines the motion of the lithium cation from an initial location ξ_1 towards a defined location ξ_2 in the lithium metal slab with a small step size of 0.0008 Å every femtosecond. Every step in this trajectory provides a free energy gradient ($\delta F/\delta \xi$), the value of the free energy gradient is obtained by averaging the dynamic trajectories over 100 fs, and the free energy ΔF is calculated as a path integral along an arbitrary path between ξ_1 and ξ_2 :¹⁰

$$\Delta F_{1-2} = \int_{\xi_1}^{\xi_2} \left(\frac{\delta F}{\delta \xi} \right) d\xi \quad (1)$$

Additional information about the method can be found in other references¹¹⁻¹³ the c-AIMD parameters used in this calculation include the use of the canonical NVT ensemble at 330K with a time step of 1 femtosecond. The Nose thermostat^{14,15} was used to keep the temperature constant with a damping parameter set to 0.5. Bader charge analysis was performed^{16,17} to study the charge in different solvent molecules.

Changes in thermodynamic properties through free energy pathway shown in Table S1 is obtain using quantum chemistry models and calculations that were performed with Gaussian16¹⁸ for the simulations and GaussView6 for visualization of the different models. Throughout all the simulations B3PW91 was selected as the hybrid exchange-correlation functional. B3PW91 is a popular method and has been used for a wide variety of different systems¹⁹⁻²². As a basis set 6-311++G(d,p) was used to describe the shape of the molecular orbitals for the models. Cluster calculations reported in this work use an implicit solvent field to approximate liquid phase results. The implicit solvation is implemented via the IEFPCM^{23,24} within the self-consistent reactive field methodology. The solvent used as a model is THF for this method but the dielectric constant were changed to better represent the electrolyte (e.g. DME= 7.2). Equations 2, 3 and 4 were used to calculate the Gibbs Free Energy of Solvation, Standard Enthalpies and Standard Molar Entropies.

$$\Delta G = G_{Total} - G_{Li^+_{gas}} - N * G_{DME_{imp}} \quad (2)$$

$$\Delta H = H_{Total} - H_{Li^+_{gas}} - N * H_{DME_{imp}} \quad (3)$$

$$T\Delta S = \Delta H - \Delta G \quad (4)$$

G_{Total} is the total Gibbs Free Energy of each solvation shell in Table S1 calculated with implicit solvation, $G_{Li^+_{gas}}$ is the Gibbs Free Energy of one lithium cation, N is the number

of solvent molecules in the solvation shell and $G_{\text{DME imp}}$ is the Gibbs Free Energy of one DME molecule in implicit solvent. (Note: in Table S1 the $G_{\text{Li}^+ \text{ gas}}$ includes the energy of the cluster of 5 Li atoms for mark 6 and cluster of 6 Li metal atoms for mark 6*)

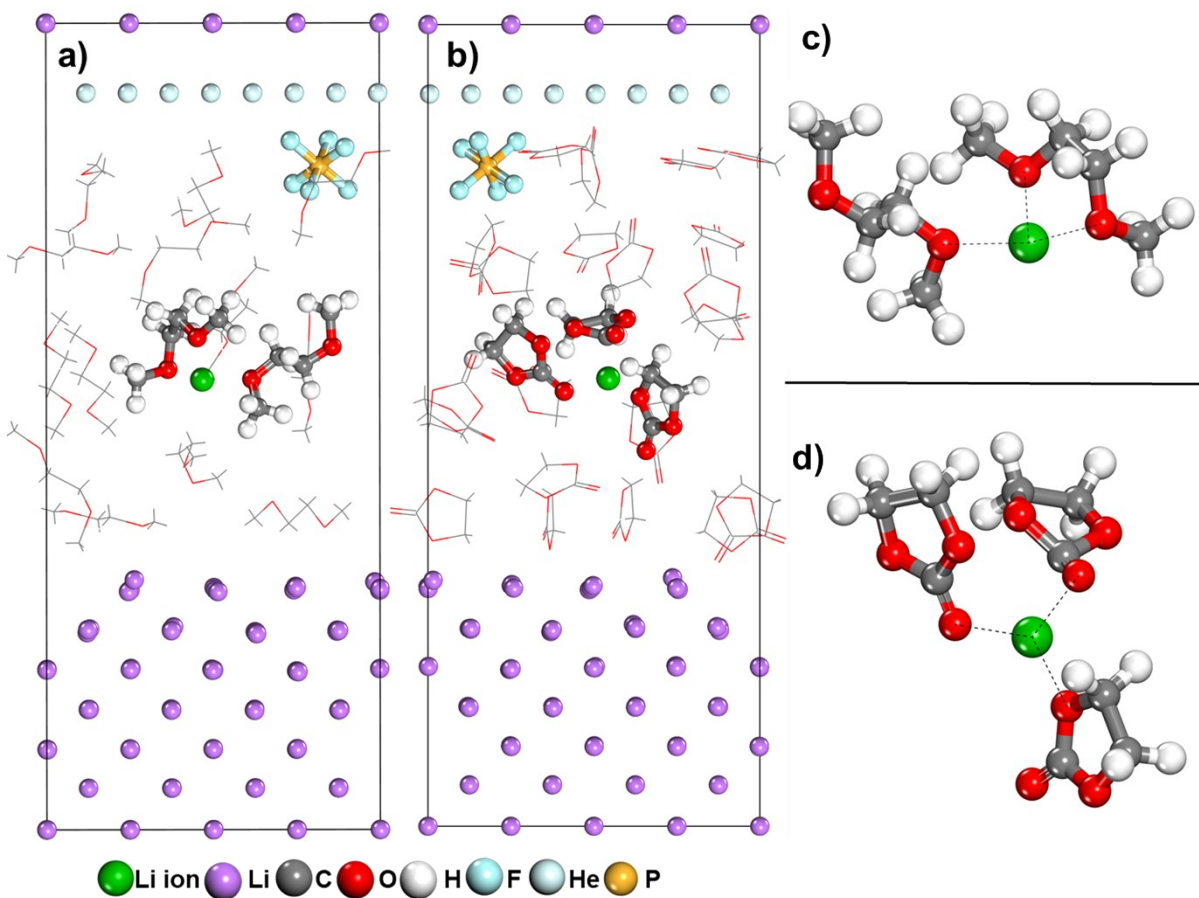


Figure S1. Initial structures. a) DME as solvent. b) EC as solvent. c) Initial solvation shell formed by 2 molecules of DME. d) Initial solvation shell formed by 3 molecules of EC

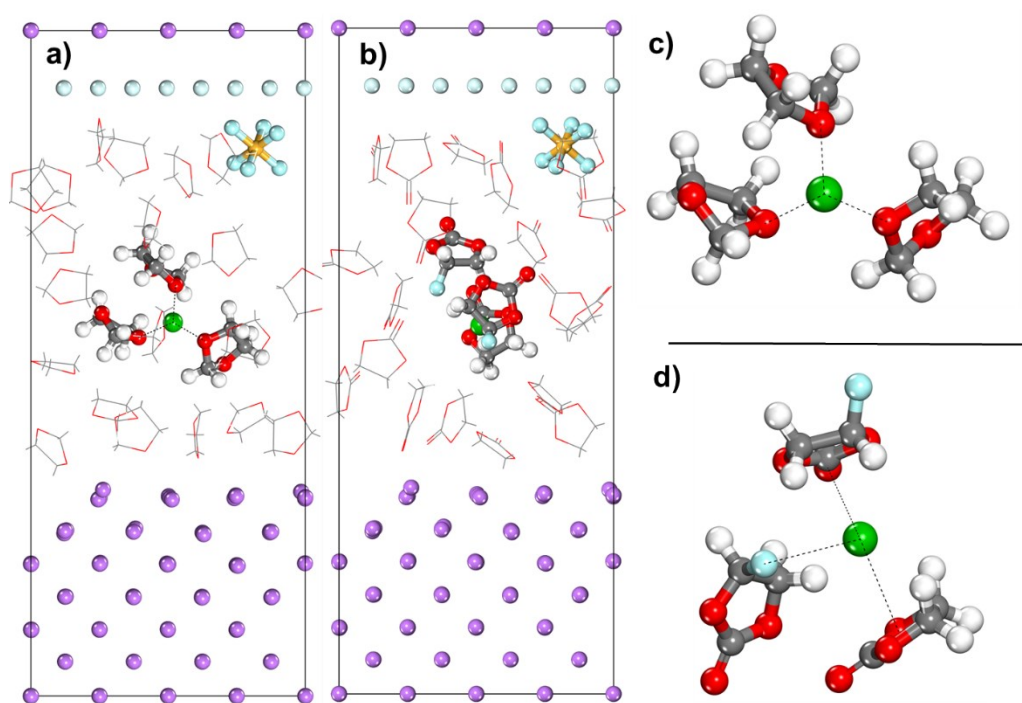


Figure S2. Initial structures. a) DOL as solvent. b) EC with FEC 10 mol% as solvent. c) Initial solvation shell formed by 3 molecules of DOL. d) Initial solvation shell formed by 1 EC and 2 FEC. Color code as Figure S1.

Figure S1 shows the color code for atoms in the molecular models: Carbon (grey), Oxygen (red), Hydrogen (white), Fluorine (yellow), Nitrogen (blue), and Lithium (purple).

Gibbs Free Energy	1	3	4	5	6	6*
$G_{\text{(Total)}} [\text{Ha}]$	-624.9033	-933.6087	-624.9161	-933.5216	-662.5876	-662.5876
$G_{\text{(Li+ gas)}} [\text{Ha}]$	-7.2924	-7.2924	-7.2924	-7.2924	-45.0668	-45.0983
$G_{\text{(N}^{\circ}\text{DME)}} [\text{Ha}]$	-617.4549	-926.1824	-617.4549	-926.1824	-617.4549	-617.4549
$\Delta G [\text{Ha}]$	-0.1560	-0.1340	-0.1688	-0.0468	-0.0659	-0.0344
$\Delta G [\text{eV}]$	-4.2447	-3.6465	-4.5930	-1.2745	-1.7927	-0.9355

Enthalpies	1	3	4	5	6	6*
$H_{\text{(Total)}} [\text{Ha}]$	-624.8353	-933.5194	-624.8520	-933.5330	-662.4988	-662.4988
$H_{\text{(Li+ gas)}} [\text{Ha}]$	-7.4464	-7.4464	-7.4464	-7.4464	-45.0119	-45.0557
$H_{\text{(N}^{\circ}\text{DME)}} [\text{Ha}]$	-617.3718	-926.0578	-617.3718	-926.0578	-617.3718	-617.3718
$\Delta H [\text{Ha}]$	-0.0171	-0.0152	-0.0338	-0.0288	-0.1151	-0.0713
$\Delta H [\text{eV}]$	-0.4642	-0.4143	-0.9196	-0.7845	-3.1319	-1.9399

Temperature	298.1500
$T\Delta S = (\Delta H - \Delta G) [\text{eV}]$	3.7805

Table S1. Changes in thermodynamic properties through free energy pathway shown in Figure 3. Full description of computed Gibbs Free Energy of Solvation, Standard Enthalpies and Standard Molar Entropies at 298 K

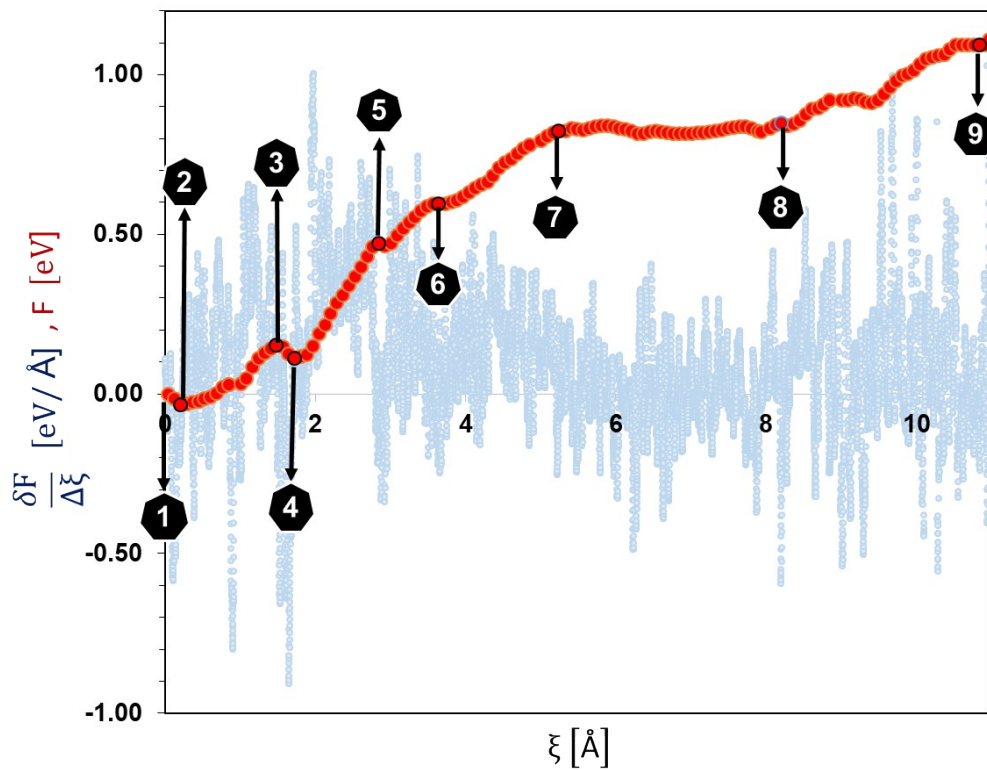


Figure S3. Free-energy profile of lithium cation diffusion and deposition in 1.0 M LiPF₆ in EC. Marks 1 through 9 highlight important events along the Li⁺ pathway.

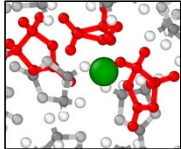
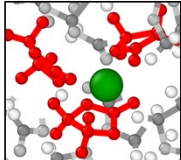
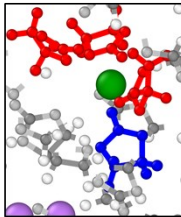
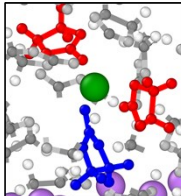
	ξ [Å]	F [eV]	ΔF [eV]	Description
	Reaction Coordinate	Free Energy	Free Energy change relative to previous step	
	0.00	0.00	0.00	Initial solvation shell 3 EC molecules (red) interacting with Li^+ through O atoms
	0.28	-0.03	-0.03	Initial solvation shell rearrangement into more stable configuration: one of the EC molecules interacts with 2 O atoms for a total of 4 O atoms in the shell
	1.40	0.14	0.17	An EC molecule (blue) close to the surface joins the solvation shell while one another leaves the shell
	1.72	0.11	-0.03	Step completes new addition of an EC molecule to the shell (blue) stabilizing the system

Figure S4. Solvation shell description found in Figure S3 (marks 1 through 4) of the Li^+ in EC with 1.0 M LiPF_6 .

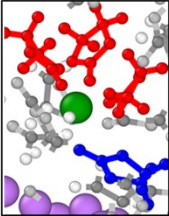
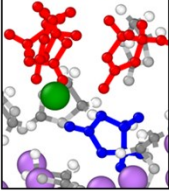
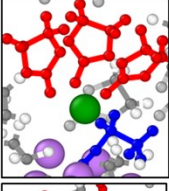
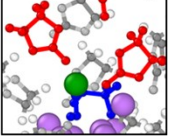
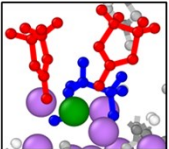
	ξ [Å]	F [eV]	ΔF [eV]	Description
	Reaction Coordinate	Free Energy	Free Energy change relative to previous step	
	2.92	0.47	0.35	The barrier represents the start of the alignment process, all molecules start to point and align with the movement of the cation towards the surface. The initial EC molecule (red) rejoins the solvation shell
	3.64	0.60	0.13	The alignment process continues driven by the cation causing the landing of the EC molecule (blue) on top of the slab as well as the dragging of the initial shell (red molecules) for its diffusion
	5.24	0.82	0.23	The molecules in the solvation shell are reduced starting by the lower EC molecule (blue)
	8.20	0.85	0.02	While the EC reduction continues, one of the EC molecules at the top leaves the shell. The cation starts interacting with the partially reduced EC and the other EC molecules are dragged to the surface
	10.84	1.09	0.25	The cation is not reduced ; instead becomes part of the SEI

Figure S5. Solvation shell description found in Figure S3 (marks 5 through 9) of the Li^+ in EC with 1.0 M LiPF_6 .

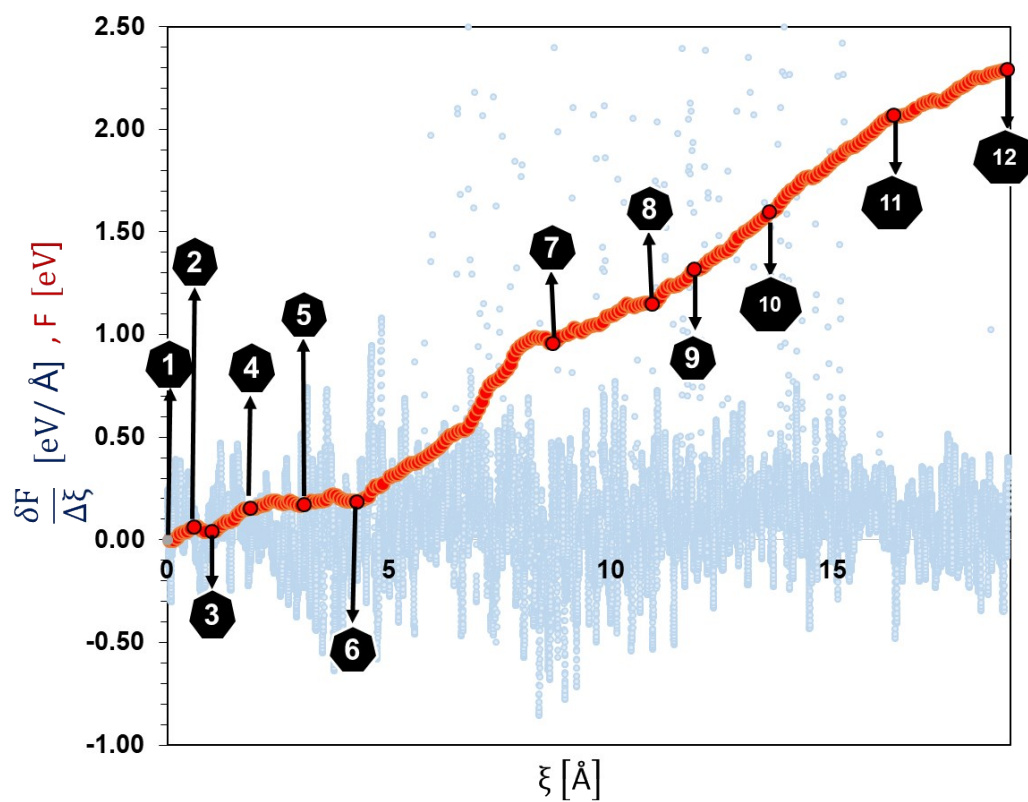


Figure S6. Free-energy profile of lithium cation diffusion and deposition in 1.0 M LiPF₆ in DOL. Marks 1 through 12 highlight important events along the Li⁺ pathway.

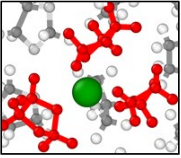
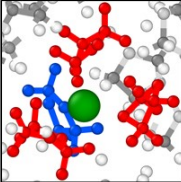
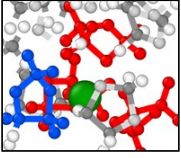
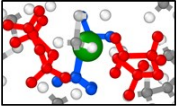
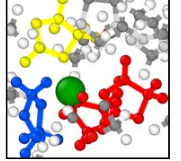
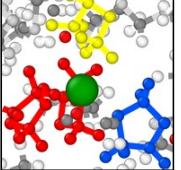
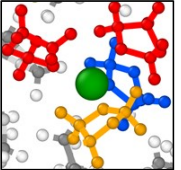
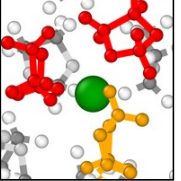
	ξ [Å]	F [eV]	ΔF [eV]	Description	
	Reaction Coordinate	Free Energy	Free Energy change relative to previous step		
1		0.00	0.00	0.00	Initial solvation shell with 3 DOL molecules (red) each interacting with 1 O atom
2		0.68	0.06	0.06	Rearrangement step to add a new DOL (blue) to the solvation shell. Barrier shown is the energy required for this DOL addition to the shell
3		1.00	0.04	-0.02	After the DOL molecule (blue) is added to the shell the system stabilizes
4		1.88	0.15	0.11	One of the initial DOL molecule (red) left the shell, and the cation remains solvated by three molecules
5		3.08	0.17	0.02	New addition of DOL molecule (yellow) to the existent shell
6		4.28	0.19	0.02	The shell remains the same while diffusing and approaching the Li metal surface
7		8.68	0.96	0.77	Free energy change represents various changes in the solvation shell, first the one DOL molecule (yellow) has left the shell while the new DOL closer to the surface joins the shell (orange)
8		10.92	1.15	0.19	Shell reconfigures to 3 molecules interacting with the cation reorienting the complex towards the surface

Figure S7. Solvation shell description found in Figure S6 (marks 1 through 8) of the Li^+ in DOL with 1.0 M LiPF_6

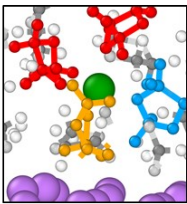
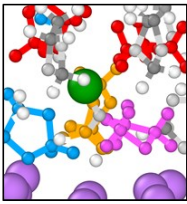
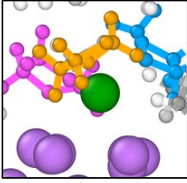
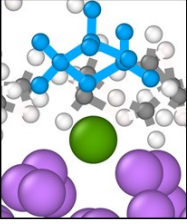
	ξ [Å]	F [eV]	ΔF [eV]	Description	
	Reaction Coordinate	Free Energy	Free Energy change relative to previous step		
9		11.96	1.32	0.17	Beginning of the cation deposition in which a new DOL molecule (turquoise) temporarily joins the solvation shell
10		13.56	1.60	0.28	New DOL molecule closer to the surface (pink) helps the deposition of the cation
11		15.96	2.01	0.41	The cation is still interacting with some of the DOL molecules closer to the surface and the beginning of desolvation
12		19.96	2.43	0.43	Li cation has been reduced and it is currently interacting only with one DOL (blue)

Figure S8. Solvation shell description found in Figure S6 (marks 9 through 12) of the Li^+ in DOL with 1.0 M LiPF_6

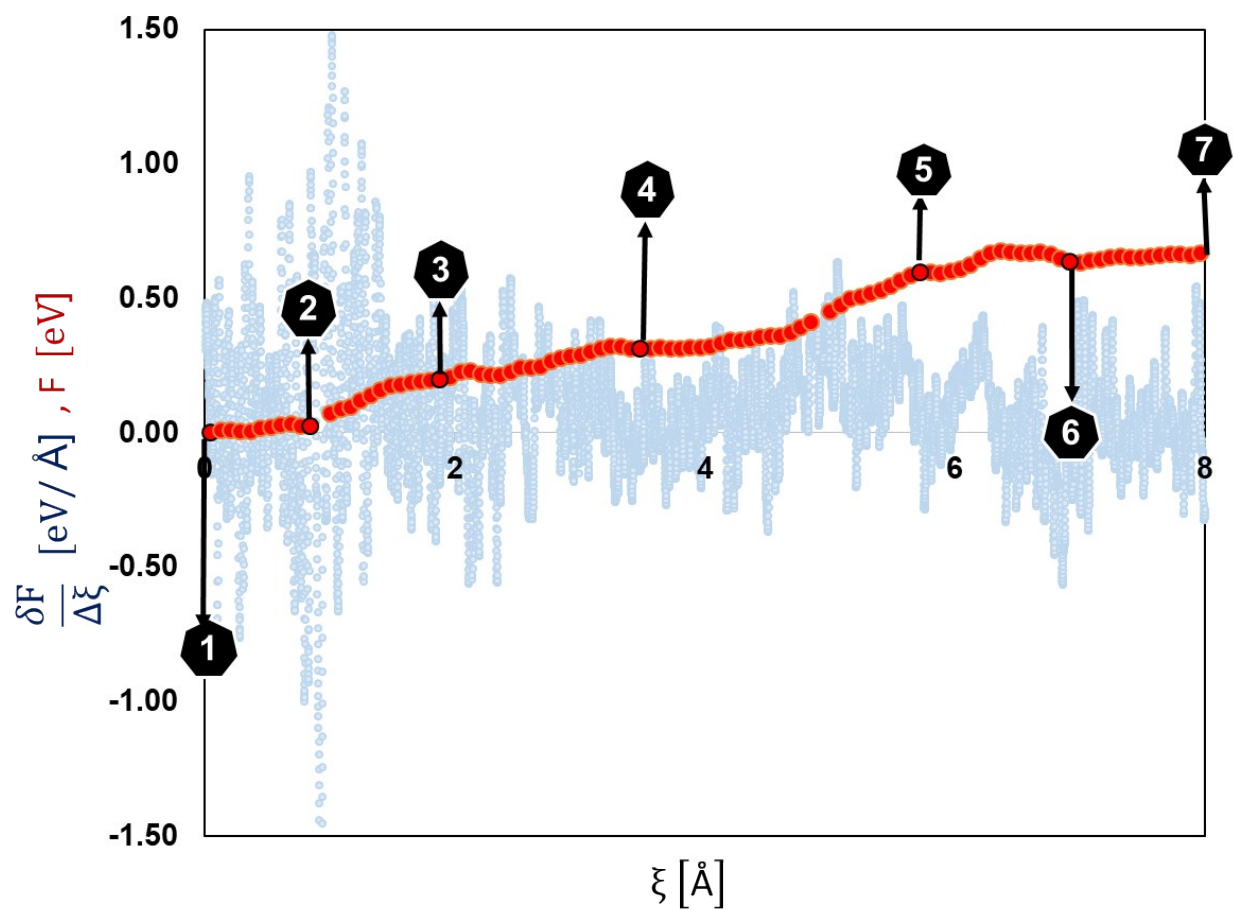


Figure S9. Free-energy profile of lithium cation diffusion and deposition in 1.0 M LiPF₆ in EC with FEC 10 mol%. Marks 1 through 7 highlight important events along the Li⁺ pathway.

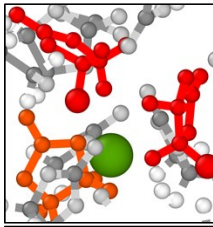
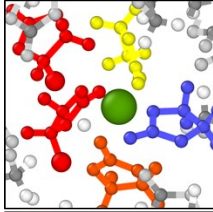
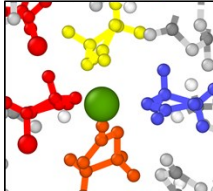
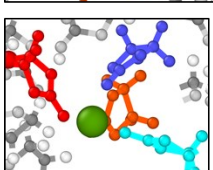
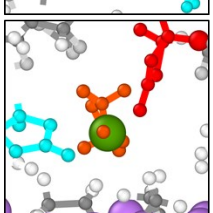
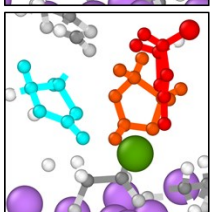
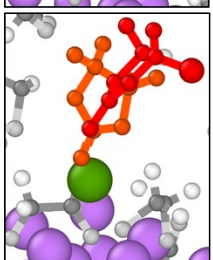
	ξ [Å]	F [eV]	ΔF [eV]	Description	
	Reaction Coordinate	Free Energy	Free Energy change relative to previous step		
1		0.00	0.00	0.00	Initial solvation shell includes 2 FEC molecules (red) and 1 EC molecule (Orange)
2		0.84	0.02	0.02	Addition of 2 new EC molecules to the shell (blue and yellow) as one FEC moves away.
3		1.88	0.20	0.18	Stabilization and diffusion of the previously formed shell, Initial FEC (red) has left completely the shell. Current shell has 1 FEC and 3 EC molecules
4		3.48	0.31	0.11	New EC molecule (turquoise) substitutes previous EC
5		5.72	0.60	0.28	Blue EC molecule leaves and the shell stabilizes to a 3 molecule shell in which one is an FEC (red)
6		6.92	0.63	0.04	Cation approaches the surface with SEI formation and alignment of the solvation shell is observed
7		7.96	0.67	0.03	Turquoise EC molecule leaves the shell as the cation starts to interact more with the nascent SEI on the surface

Figure S10. Solvation shell description found in Figure S9 (marks 1 through 7) of the Li^+ in 1.0 M LiPF_6 in EC with FEC 10 mol%

References

- (1) Camacho-Forero, L. E.; Smith, T. W.; Bertolini, S.; Balbuena, P. B. Reactivity at the Lithium-Metal Anode Surface of Lithium-Sulfur Batteries. *J. Phys. Chem. C* **2015**, *119*, 26828-26839.
- (2) Maple, J. R.; Dinur, U.; Hagler, A. T. DERIVATION OF FORCE-FIELDS FOR MOLECULAR MECHANICS AND DYNAMICS FROM ABINITIO ENERGY SURFACES. *Proc. Natl. Acad. Sci. U. S. A.* **1988**, *85*, 5350-5354.
- (3) Kresse, G.; Furthmuller, J. Efficiency of ab-initio total energy calculations for metals and semiconductors using a plane-wave basis set. *Computational Materials Science* **1996**, *6*, 15-50.
- (4) Kresse, G.; Hafner, J. Ab initio molecular dynamics for liquid metals. *Physical Review B* **1993**, *47*, 558.
- (5) Kresse, G.; Hafner, J. Ab initio molecular-dynamics simulation of the liquid-metal-amorphous-semiconductor transition in germanium. *Physical Review B* **1994**, *49*, 14251-14269.
- (6) Blöchl, P. E. Projector augmented-wave method. *Physical review B* **1994**, *50*, 17953.
- (7) Kresse, G.; Joubert, D. From ultrasoft pseudopotentials to the projector augmented-wave method. *Physical Review B* **1999**, *59*, 1758-1775.
- (8) Perdew, J. P.; Burke, K.; Ernzerhof, M. Generalized Gradient Approximation Made Simple. *Physical Review Letters* **1996**, *77*, 3865-3868.
- (9) Monkhorst, H. J.; Pack, J. D. Special points for Brillouin-zone integrations. *Physical Review B* **1976**, *13*, 5188-5192.
- (10) Bucko, T. Ab initio calculations of free-energy reaction barriers. *Journal of Physics: Condensed Matter* **2008**, *20*, 064211.
- (11) Komeiji, Y. Implementation of the blue moon ensemble method. *Chem-bio Informatics Journal* **2007**, *7*, 12-23.
- (12) Ciccotti, G.; Ferrario, M. Blue Moon Approach to Rare Events. *Molecular Simulation* **2004**, *30*, 787-793.
- (13) Cheng, T.; Xiao, H.; Goddard, W. A. Free-Energy Barriers and Reaction Mechanisms for the Electrochemical Reduction of CO on the Cu(100) Surface, Including Multiple Layers of Explicit Solvent at pH 0. *The Journal of Physical Chemistry Letters* **2015**, *6*, 4767-4773.
- (14) Nosé, S. A unified formulation of the constant temperature molecular dynamics methods. *The Journal of Chemical Physics* **1984**, *81*, 511-519.
- (15) Hoover, W. G. Canonical dynamics: Equilibrium phase-space distributions. *Physical Review A* **1985**, *31*, 1695-1697.
- (16) Tang, W.; Sanville, E.; Henkelman, G. A grid-based Bader analysis algorithm without lattice bias. *Journal of Physics: Condensed Matter* **2009**, *21*, 084204.
- (17) Henkelman, G.; Arnaldsson, A.; Jónsson, H. A fast and robust algorithm for Bader decomposition of charge density. *Computational Materials Science* **2006**, *36*, 354-360.
- (18) Frisch, M. J.; Trucks, G. W.; Schlegel, H. B.; Scuseria, G. E.; Robb, M. A.; Cheeseman, J. R.; Scalmani, G.; Barone, V.; Petersson, G. A.; Nakatsuji, H.; Li, X.; Caricato, M.; Marenich, A. V.; Bloino, J.; Janesko, B. G.; Gomperts, R.; Mennucci, B.; Hratchian, H. P.; Ortiz, J. V.; Izmaylov, A. F.; Sonnenberg, J. L.; Williams; Ding, F.; Lipparini, F.; Egidi, F.; Goings, J.; Peng, B.; Petrone, A.; Henderson, T.; Ranasinghe, D.; Zakrzewski, V. G.; Gao, J.; Rega, N.; Zheng, G.; Liang, W.; Hada, M.; Ehara, M.; Toyota, K.; Fukuda, R.; Hasegawa, J.; Ishida, M.; Nakajima, T.; Honda, Y.; Kitao, O.; Nakai, H.; Vreven, T.; Throssell, K.; Montgomery Jr., J. A.; Peralta, J. E.; Ogliaro, F.; Bearpark, M. J.; Heyd, J. J.; Brothers, E. N.; Kudin, K. N.; Staroverov, V. N.; Keith, T. A.; Kobayashi, R.; Normand, J.; Raghavachari, K.; Rendell, A. P.; Burant, J. C.; Iyengar, S. S.; Tomasi, J.; Cossi, M.; Millam, J. M.; Klene, M.; Adamo, C.; Cammi,

R.; Ochterski, J. W.; Martin, R. L.; Morokuma, K.; Farkas, O.; Foresman, J. B.; Fox, D. J.: Gaussian 16 Rev. C.01. Wallingford, CT, 2016.

(19) Camacho-Forero, L. E.; Smith, T. W.; Bertolini, S.; Balbuena, P. B. Reactivity at the Lithium–Metal Anode Surface of Lithium–Sulfur Batteries. *The Journal of Physical Chemistry C* **2015**, *119*, 26828-26839.

(20) Jung, H. M.; Park, S.-H.; Jeon, J.; Choi, Y.; Yoon, S.; Cho, J.-J.; Oh, S.; Kang, S.; Han, Y.-K.; Lee, H. Fluoropropane sultone as an SEI-forming additive that outperforms vinylene carbonate. *Journal of Materials Chemistry A* **2013**, *1*, 11975-11981.

(21) Jalbout, A. F.; Nazari, F.; Turker, L. Gaussian-based computations in molecular science. *Journal of Molecular Structure: THEOCHEM* **2004**, *671*, 1-21.

(22) Curtiss, L. A.; Redfern, P. C.; Raghavachari, K.; Pople, J. A. Assessment of Gaussian-2 and density functional theories for the computation of ionization potentials and electron affinities. *The Journal of Chemical Physics* **1998**, *109*, 42-55.

(23) Tomasi, J.; Mennucci, B.; Cammi, R. J. C. r. Quantum mechanical continuum solvation models. **2005**, *105*, 2999-3094.

(24) Pascual-ahuir, J.-L.; Silla, E.; Tunon, I. J. J. o. C. C. GEPOL: An improved description of molecular surfaces. III. A new algorithm for the computation of a solvent-excluding surface. **1994**, *15*, 1127-1138.